JOURNAL OF GEOPHYSICAL RESEARCH, VOL. 111, A11S03, doi:10.1029/2006JA011690, 2006

Storm time evolution of the outer radiation belt: Transport and losses

A. Y. Ukhorskiy,[1] B. J. Anderson,[1] P. C. Brandt,[1] and N. A. Tsyganenko[2]

Received 2 February 2006; revised 31 August 2006; accepted 12 September 2006; published 1 November 2006.

[1] During geomagnetic storms the magnetic field of the inner magnetosphere exhibits large-scale variations over timescales from minutes to days. Being mainly controlled by the magnetic field the motion of relativistic electrons of the outer radiation belt can be highly susceptible to its variations. This paper investigates evolution of the outer belt during the 7 September 2002 storm. Evolution of electron phase space density is calculated with the use of a test-particle simulation in storm time magnetic and electric fields. The results show that storm time intensification of the ring current produces a large impact on the belt. In contrast to the conventional D_{st} effect the dominant effects are nonadiabatic and lead to profound and irreversible transformations of the belt. The diamagnetic influence of the partial ring current leads to expansion of electron drift orbits such that their paths intersect the magnetopause leading to rapid electron losses. About 2.5 hr after the storm onset most of the electrons outside $L = 5$ are lost. The partial ring current pressure also leads to an electron trap in the dayside magnetosphere where electrons stay on closed dayside drift orbits for as long as 11 hours. These sequestered electrons are reinjected into the outer belt due to partial recovery of the ring current. The third adiabatic invariant of these electrons exhibits rapid jumps and changes sign. These jumps produce localized peaks in the L^*-profile of electron phase space density which have previously been considered as an observable indication of local electron acceleration.

Citation: Ukhorskiy, A. Y., B. J. Anderson, P. C. Brandt, and N. A. Tsyganenko (2006), Storm time evolution of the outer radiation belt: Transport and losses, *J. Geophys. Res.*, *111*, A11S03, doi:10.1029/2006JA011690.

1. Introduction

[2] Earth's outer electron belt consists of relativistic ($\gtrsim$1 MeV) electrons trapped in geomagnetic field at $L \gtrsim 3$. Electron fluxes in the belt exhibit a nonlinear response to geomagnetic activity. Flux levels after a storm may increase, decrease or stay the same compared to their prestorm values [*Reeves et al.*, 2003]. During storms, however, electron flux behavior is more consistent: spacecraft observations show a decrease in flux intensity at the main phase of most of the storms. This storm time dropout of relativistic electron fluxes has yet to be explained. In particular, it is not clear to what extent the observed dropout is a result of adiabatic inflation of the inner magnetospheric field due to growth of ring current intensity and to what extent it is caused by losses due to magnetopause shadowing and or precipitation. The goal of this paper is to identify transport and loss mechanisms related to the large-scale storm time magnetic field that drive global evolution of the outer electron belt during large geomagnetic storms.

[3] In a time-varying geomagnetic field, relativistic electrons can exhibit three distinct quasi-periodic motions associated with adiabatic invariants (μ, J, Φ). In the absence of field fluctuations in resonance with any of these motions, electron dynamics is mainly controlled by the magnetic field. Most of the plasma pressure in the inner magnetosphere is carried by the ring current, which distorts the magnetic field and affects electron drift motion. A close relationship between the ring current and the outer radiation belt was established by early spacecraft observations [*Dessler and Karplus*, 1960, 1961; *McIlwain*, 1966], suggesting that a decrease of electron flux levels during storm main phase could be attributed to the adiabatic response of relativistic electrons to a slow (compared to electron drift period) increase in ring current intensity. An increase in ring current intensity decreases the magnetic flux Φ enclosed by an electron drift orbit. To conserve Φ under increased ring current intensity, the electron must move outward to a region of lower magnetic field intensity. Since $\mu = p_\perp^2/2mB$ is also conserved, the outward motion decreases the electron energy. Thus after an increase in ring current intensity, measurements of electrons within a fixed energy at a fixed radial location will register electrons previously located at lower radial distances where their energy was higher and their phase space density lower so that a lower flux is measured.

[1] Johns Hopkins University Applied Physics Laboratory, Laurel, Maryland, USA.
[2] Universities Space Research Association, NASA Goddard Space Flight Center, Greenbelt, Maryland, USA.

0148-0227/06/2006JA011690$09.00

[4] Since the ring current intensity is most often monitored by the D_{st} index, the fully adiabatic effect on radiation belt electrons produced by its increase is commonly referred to as the " D_{st} effect." While the D_{st} effect is generally believed to be the dominant cause of electron flux dropouts at storm main phase, some observational studies [e.g., *Li et al.*, 1997] indicate that some of the flux decrease at higher L must be nonadiabatic, e.g., dominated by losses.

[5] To differentiate among adiabatic and nonadiabatic mechanisms of the electron flux dropouts during storms, one must follow the full spatiotemporal evolution of electron phase space density (PSD). This requires the use of global models of the electron belt. Most of the existing radiation belt models, however, are based on a dipole [*Jordanova and Miyoshi*, 2005], empirical [*Fok et al.*, 2001], or global MHD models [*Elkington et al.*, 2004] of the geomagnetic field which do not have a realistic representation of storm time ring current, particularly its asymmetry, and therefore cannot accurately describe global evolution of the magnetic field and hence the electron belt drift orbits during storms.

[6] Recently, *Ukhorskiy et al.* [2006] developed a new technique for calculating the inductive electric field corresponding to time evolution of geomagnetic field models and implemented it for the *Tsyganenko and Sitnov* [2005] (TS05) magnetic field model. The TS05 model was specifically designed for realistic representation of the inner magnetospheric magnetic field during disturbed conditions including strong influence of both the symmetric and asymmetric or partial ring current. Complemented with the inductive electric field the TS05 yields a self-consistent description of the inner magnetospheric fields suitable for modeling storm time evolution of the outer radiation belt.

[7] In this paper the TS05 model with the inductive electric field is used in a test particle simulation of the outer radiation belt during the 7 September 2002 geomagnetic storm selected for analysis by GEM IM/S campaign. Geomagnetic storms of 3–15 September 2002 time period were used by *Tsyganenko and Sitnov* [2005] for the out-of-sample model validation (see Figure 6 and Table 5 of their paper). It was shown that the cross correlation coefficient of the observed and modeled D_{st} indices is high, 0.96, which proves that the TS05 magnetic field model well captures the overall storm dynamics during that time period.

[8] Our test-particle simulation shows that storm time partial ring current produces large non-adiabatic and therefore irreversible effects on the electron belt. In particular, a strong nightside depression of geomagnetic field leads to rapid electron losses by opening previously closed drift paths to the magnetopause; all electrons from $L > 5$ are lost in about 2.5 hours after the storm onset. Because the duskside depression is due to the partial or asymmetric ring current, the actual nightside ion pressure and corresponding magnetic field distortion are much larger than one would estimate from D_{st} assuming a symmetric ring current.

[9] In addition to this prompt loss, the partial ring current diamagnetic effect also yields localized extrema in the magnetic field corresponding to magnetic drift path islands. These islands temporarily trap a small fraction of the radiation belt electrons yielding local maxima in the radial PSD profile. This process occurred twice during the storm, once in the evening where the "trapped" island population was transient and subsequently lost, and later on the dayside. The dayside maximum in magnetic field intensity corresponded to a small island of closed drift orbits that sequestered a small fraction of the radiation belt electrons in $\sim 1-3\ R_E$ region of the dayside magnetosphere. Electrons remained trapped in this dayside island throughout most of the storm ($\sim$11 hours) until the ring current recovers and the electrons are reinjected into the belt. The third adiabatic invariant Φ of electrons that populate these islands exhibits rapid jumps and even changes sign. If electron PSD is computed as a function of L^*, this "trapping" process results in localized peaks in the PSD profile at $L^* \sim 4-5$.

[10] The next section describes the details of our radiation belt model. In section 3 we describe the evolution of electron PSD during the 7 September 2002 storm. Section 4, followed by conclusions, discusses the implications of strong nonadiabaticity of electron motion during the storm for our understanding of radiation belt storm time dynamics.

2. Radiation Belt Model

[11] Owing to their low density, relativistic electrons of the outer belt do not produce a significant feedback onto magnetospheric fields. The electron belt can therefore be described with a test-particle approach. In this paper we use the Vlasov Hybrid Simulation method [*Nunn*, 1993] in which the phase space of the system is populated by a large number of electrons (test particles) whose motion is traced separately in time-varying electric $\mathbf{E}(t)$ and magnetic $\mathbf{B}(t)$ fields. At simulation start, each test particle is prescribed with an initial value of PSD $f(\mathbf{r}, \mathbf{p}, t = 0)$, which according to the Liouville's theorem is conserved along the particle's phase space trajectory: $\mathbf{r} = \mathbf{r}(t)$, $\mathbf{p} = \mathbf{p}(t)$. At a given moment of time the PSD of radiation belt electrons is calculated by interpolating $f(\mathbf{r}(t), \mathbf{p}(t), t)$ from test particle locations on a regular grid. This yields an estimate of the solution of the Vlasov equation and therefore provides the fully kinetic description of the electron belt.

[12] In the analysis of the storm time evolution of the belt, we consider variations of magnetospheric fields only on the time scales of 5 min and longer, which do not violate either the first (μ) or second (J) invariants of the relativistic electrons. (Note that a typical bounce period for an MeV electron is on the order of a second or less.) The electron motion can therefore be described in the guiding center approximation. To simplify calculations and save computational time we restricted consideration to equatorial (90°, $J = 0$) electrons. Since both the first and second invariants are conserved, the fundamental dynamics of equatorial and nonequatorial electrons should be the same, and this calculation should capture the key aspects of the full three-dimensional motion. The guiding center motion of an equatorial electron can be written as [*Northrop*, 1963]:

$$\begin{cases} \dfrac{d\mathbf{r}}{dt} = c\dfrac{\mathbf{E}\times\hat{b}}{B} + \dfrac{\mu c}{\gamma e}\dfrac{\hat{b}\times\nabla B}{B} \\ \mu = \dfrac{p^2}{2mB} = const \end{cases} \tag{1}$$

where $\hat{b} = \mathbf{B}/B$, γ is the relativistic factor, c is the speed of light, $\mathbf{r}$ is the position of the guiding center of the electron, m, e, and p are its mass, charge, and momentum.

[13] From (1) it follows that electron motion is specified completely by external magnetic and electric fields. Thus in modeling the evolution of the electron belt during large storms it is critical to use an accurate description of the inner magnetospheric fields valid during disturbed geomagnetic activity. The motion of equatorial electrons consists of the $\mathbf{E} \times \mathbf{B}$ (first term) and the gradient (second term) drifts. Owing to its energy dependence, the gradient drift term generally dominates over the $\mathbf{E} \times \mathbf{B}$ term for relativistic energies far from drift resonances. Thus simulation accuracy is especially sensitive to the accuracy of magnetic field model.

[14] In our model the time-dependent magnetic field is derived from the TS05 magnetic field model, which is specifically designed to represent the realistic magnetic field during storms. The TS05 model is driven by ten control parameters: P_{dyn}, D_{st} index, the B_y and B_z components of the interplanetary magnetic field, and six variables W_k, which describe individual field sources as time-varying functions of geoeffective solar wind parameters (for details, see *Tsyganenko and Sitnov* [2005]). TS05 can be used as a dynamical model, since its control parameters depend on the current value and the history of solar wind conditions.

[15] The electric field in the magnetospheric plasma has an inductive and and a potential component. The inductive component corresponding to time-varying output of the TS05 model, is calculated from the expression:

$$\mathbf{E}(\mathbf{r},t) = -\frac{1}{4\pi c}\frac{\partial}{\partial t}\int_V d^3r' \frac{\mathbf{B}(\mathbf{r}',t)\times(\mathbf{r}-\mathbf{r}')}{|\mathbf{r}-\mathbf{r}'|^3}, \qquad (2)$$

which yields an estimate of the solution of the Faraday's law equation: $c\nabla \times \mathbf{E} = -\partial_t \mathbf{B}$ (for details, see *Ukhorskiy et al.* [2006]). It has to be noted, that being a statistical model, TS05 assumes spatial coherence over the whole computational domain and therefore does not describe wave phenomena. Thus the model can account only for field variations on time scales longer than the time, 1–3 min, for the fast mode wave to propagate through the inner magnetosphere.

[16] The potential electric field however does not usually exhibit substantial variations on the time scale of electron drift and does not have amplitude large enough to produce a substantial impact on electron motion. However, for the sake of generality our model includes a time-dependent potential electric field derived from the *Volland* [1973] *Kp*-driven expression for the electric field of large-scale magnetospheric convection.

[17] Throughout the paper, three different parameters are used for quantifying the electron PSD radial profile in the belt. The first is the normalized radial distance $L = r/R_E$. The second is the generalized L parameter [*Roederer*, 1970]: $L^* = -2\pi B_0 R_E^2/\Phi$, where B_0 is the magnetic field intensity at the magnetic equator on the Earth, R_E is Earth's radius. The expression for L^* converts the third invariant Φ to units of dimensionless length. Thus L^* is suitable for calculating a coarse-grained PSD $f(L^*) = \frac{1}{2\pi}\int_0^{2\pi} f(L^*(\Phi), \varphi)d\varphi$, which is often used in the Fokker-Plank description of electron transport in the belt [e.g., *Schultz and Lanzerotti*, 1974]. The third is $\mathcal{L} = (B_0/B)^{1/3}$. Since in a steady state case, equatorial electrons drift along contours of $B = const$, $\mathcal{L}$ is convenient for calculating PSD profiles in slow varying magnetic configurations for which $\mathcal{L} \simeq L^*$ [*Elkington et al.*, 2003]. It should be noted, however, that while in a dipole field $L = L^* = \mathcal{L}$, in the case of a strongly disturbed magnetic configuration, the thee parameters can have substantially different values: $L \neq L^* \neq \mathcal{L}$.

3. Storm Time Evolution of the Outer Belt

[18] In this section we discuss the results of a test-particle simulation of the outer electron belt during the 7 September 2002 geomagnetic storm. During this storm the D_{st} index dropped below −160 nT. During a moderately strong storm such as this, the distribution of magnetic field intensity in the inner magnetosphere can change significantly.

[19] To represent the state of the inner magnetospheric magnetic field, we use equatorial contours of constant magnetic field intensity, which also specify steady-state drift trajectories of equatorial electrons. Thus, the topology of these contours directly reflects drift dynamics of relativistic electrons. For quiet conditions there are no local extrema in the field intensity above the Earth so that the constant-B contours are equivalent to the contours of a dipole field in that there is a continuous non-singular transformation relating contours of these two fields. The interiors of all the quiet time contours include the origin where fields exhibit singularity. By contrast, during storm main phase, an increase in ring current intensity yields local extrema in the field intensity, which change the topology of constant-B contours, resulting in new types of contours that close on themselves but do not encompass the Earth. In the paper such magnetic field regions are referred to as "magnetic drift path islands."

[20] An example of a disturbed geomagnetic field with magnetic drift path islands is shown in Figure 1. Figure 1a of the figure shows the distribution of equatorial magnetic field obtained from the TS05 model for the 7 September 2002 storm when D_{st} approached its minimum. Two magnetic drift path islands are indicated with red dotted lines. Formation of these magnetic drift path islands is illustrated in Figure 1b, which shows radial profiles of the equatorial field intensity calculated along the $y = z = 0$ line. While the quiet time profile drops monotonically with radial distance, during disturbed conditions diamagnetic effect due to partial ring current yields localized minimum and maximum in the profile which result in the dayside and the nightside islands shown in Figure 1a. Since the drift motion of energetic electrons is mainly driven by the magnetic field, it can be expected that topological changes in the field accompanied by formation and disappearance of magnetic drift path islands can have a strong impact on the outer electron belt.

[21] To assess the dominant loss and transport mechanisms during storm main phase, we included only the electron population, that existed prior to the storm onset. All external sources of relativistic electrons that can mask internal acceleration and loss processes were neglected. To visualize the global evolution of the belt, we considered a slice of the electron PSD at μ = 2300 MeV/G, which in a dipole field corresponds to 2 MeV electrons at geosynchronous orbit. For initial conditions we took a solution of the steady state radial diffusion equation with an electron lifetime τ of 1 day and the *Brautigam and Albert* [2000]

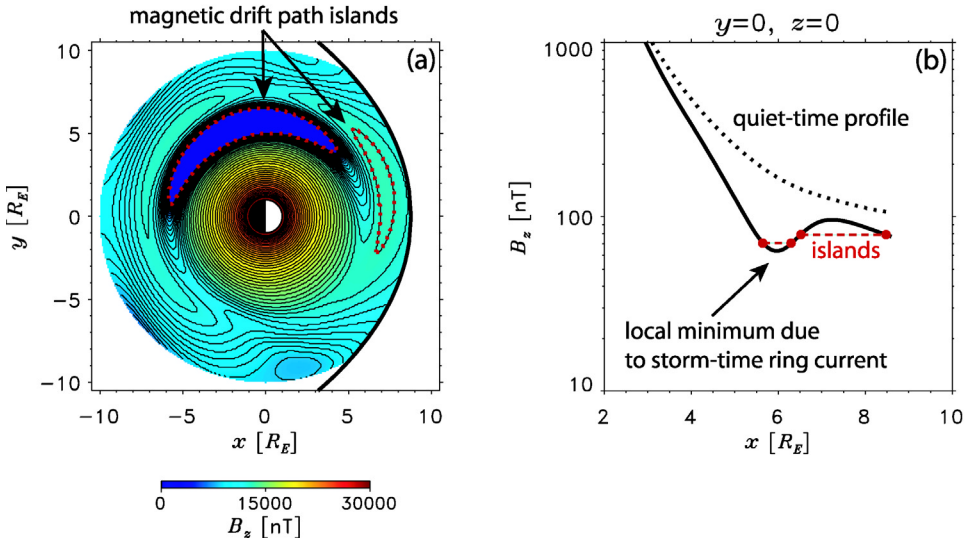

Figure 1. Storm time magnetic field from the TS05 model. (a) Distribution of magnetic field intensity at the magnetic equator. The nightside and the dayside magnetic drift path islands are shown with the red dotted line. (b) Comparison of a quiet time (dotted line) and storm time (solid line) profiles of magnetic field intensity. Red dotted line shows the location of the dayside and the nightside islands shown in Figure 1a.

diffusion coefficient at $Kp = 2$. These conditions are often taken as initial conditions in radial diffusion models of transport in the belt [e.g., *Shprits and Thorn*, 2004].

[22] The simulation was started with 10^5 test particles evenly distributed in the computational domain ($r < 10R_E$). Evolution of electron PSD was computed by interpolating the PSD values at particle locations on a regular grid with a resolution of 0.25 R_E. Time varying electric end magnetic fields used for pushing the particles were put on the same grid. To calculate the guiding center motion of the particles equations (1) were integrated with the use of the fourth-order Runge-Kutta method with an adaptive stepsize control [*Press et al.*, 1992]. To verify whether the guiding center approximation holds along particle trajectories we used a numerical criterion similar to the stable trapping criterion [*Chirikov*, 1987]. Particles who failed the criterion were removed from the simulation. By the end of the simulation less then 10% of test particles failed the criterion, which justifies the use of the guiding center approximation. Particles who escaped the computational domain or were magnetopause lost were also removed from the simulation. Less then 10^3 test particles were left in the computational domain by the end of the simulation.

[23] The simulation results are summarized in Figure 2. Time series of solar wind dynamic pressure (P_{dyn}) and the D_{st} index during the simulated portion of the storm are shown in the top two panels. The simulated period is divided into six intervals according to the state of the electron belt as reflected in the simulated PSD distribution. The bottom three panels in Figure 2 show snapshots at the beginning of each interval of the electron PSD, the magnetic field, and radial profile of the electron PSD. The top series of plots are snapshots of equatorial distribution of the electron PSD at $\mu = 2300$ MeV/G with magnitude indicated with color. The middle set of plots shows snapshots of magnetic field intensity, indicated with color, at the equator with overplotted constant-B contours. Snapshots of the radial profile of electron PSD calculated as $f(\mathcal{L}) = \frac{1}{2\pi}\int_0^{2\pi} d\varphi f(\mathcal{L}, \varphi)$ are show in the bottom panel.

[24] Snapshots in the first column (interval 1) show the initial conditions. Contours of constant B indicate typical quiet-time conditions: a quasi-dipole magnetic field compressed on the dayside. Initial distribution of electron PSD was normalized such that $\max(f) = 1$.

[25] The initial conditions persist without any substantial change until the interplanetary shock arrives (interval 2). A rapid increase in P_{dyn} associated with the shock moves the magnetopause inward, which results in immediate electron losses from the outermost L shells.

[26] Interval 3 corresponds to the initial growth of the ring current. At the start of the interval the partial ring current is strong enough to form a magnetic minimum and corresponding drift path island in the nightside premidnight sector (see the magnetic field snapshot). Since electrons tend to drift along constant-B contours, such magnetic drift path islands act as electron traps. The trapped electron population can be seen in the upper snapshot at the location of the nightside island. Electrons stayed trapped here for about 30 minutes when, due to continuous intensification of the ring current, the drift paths changed, releasing these particles to open drift paths so that they were lost by the end of interval 3.

[27] After the initial inward displacement due to the shock arrival, the magnetopause location does not change substantially through the duration of intervals 3 and 4. Most of the electron loss during these intervals is associated with a continuous growth in the ring current intensity. According to the TS05 model ring current intensity peaks around $L \simeq 5$. Its growth leads to a diamagnetic effect; constant-B contours located inward of the maximum are pushed further in, while the contours outward of the maximum expend and eventually cross the magnetopause.

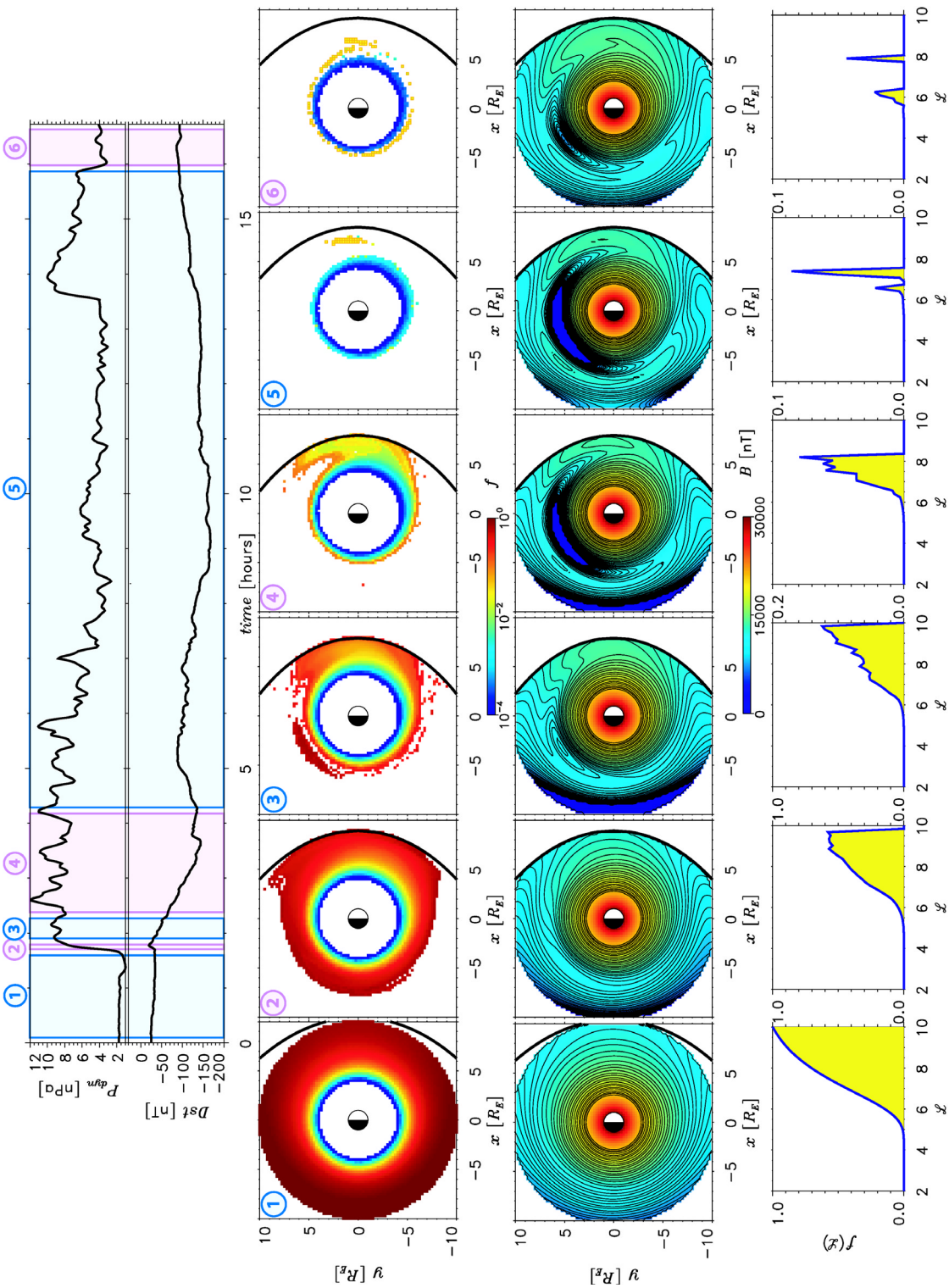

Figure 2. Test-particle simulation of the outer electron belt during the 7 September 2002 geomagnetic storm. Two top panels: time series of solar wind P_{dyn} and D_{st} index passed through the moving average filter with a 5-min window and used as first two inputs of the TS05 model. Three bottom panels: phase space density of $\mu = 2.3\ 10^3$ MeV/G electrons, equatorial magnetic field, and radial profiles of coarse-grained phase space density $f(\mathcal{L})$ during six time intervals indicated with color boxes at the top panel.

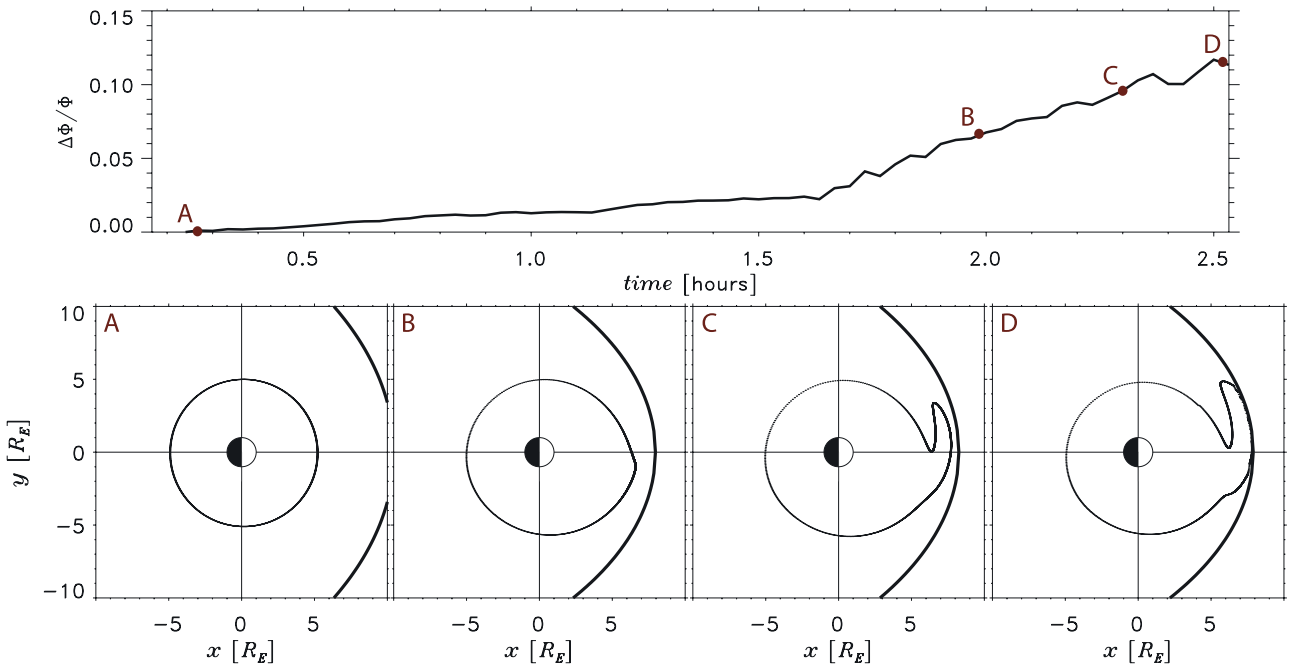

Figure 3. Storm time expansion of the relativistic electron drift orbit leading to electron escape through the magnetopause. (top) Relative change of the third adiabatic invariant. (bottom) (a) Electron orbit before the storm onset, (b,c) during initial partial ring current growth, (d) prior to electron loss through the magnetopause.

As a result particles previously located at closed drift orbits are transferred into open orbits and get lost.

[28] Expansion of electron drift trajectories with the subsequent loss through the magnetopause due to storm time intensification of the partial ring current is illustrated in Figure 3. It shows the evolution of the drift orbit for a test particle initially located at $L \simeq 5$ outside of the partial ring current maximum. The bottom panel shows steady state drift trajectories before the storm onset (A), during initial ring current enhancement (A and B), and prior to the electron escape through the magnetopause (D). Relative change in the third adiabatic invariant of the particle is shown in the upper panel. It follows that the drift orbit expansion is not fully adiabatic; a 12% change in the third invariant is observed prior to the electron loss.

[29] At the beginning of interval 5 (~2.5 hr after the storm onset) most of the electrons from $L > 5$ are lost (note a change in scale on the vertical axis in the third panel of Figure 2). The electron drainage obtained here is more pronounced than anticipated by earlier work. The reason for this is that the partial ring current is longitudinally localized so that its effectiveness in distorting and opening electron drift paths is out of proportion to its contribution to the D_{st} index. Hence, D_{st} is not indicative of the true partial "inflation" effected by the partial ring current. Estimates of inflation based on D_{st} and assuming a symmetric pressure distribution therefore dramatically underestimate this loss.

[30] The severity of the loss due to the strong asymmetric ring current would appear to leave little room for the adiabatic recovery of relativistic electron fluxes after the storm. It therefore suggests that the outer belt electrons following major storms are a new population rather than the reappearance of the original outer belt particles. If, as these results imply, the pre-storm outer belt is essentially removed during storm main phase, then the post-storm outer belt is not related to the old outer belt, but is a new population whose source and mechanism of transport we do not address here. If the two populations are distinct it may then be easier to understand why there is so little apparent relationship between the prestorm and poststorm outer belt flux levels [*Reeves et al.*, 2003].

[31] The electrons that remain in the outer magnetosphere at the beginning of interval 5 are those relatively few that became trapped in a magnetic drift path island on the dayside. The dayside island remains stable and holds electrons throughout most of the storm main phase (~11 hours). The dayside island collapses at the start of interval 6 when the ring current intensity decreases and the trapped populations are transferred back to quasi-circular orbits and resume their drift motion around the Earth. To the best of our knowledge the existence of such a stable population of trapped electrons has not been observed in previous simulations of the belt owing to the fact that it depends on a realistic representation of the magnetic field distortion due to the asymmetric storm time ring current. In the next section we discuss the implications of electron trapping for analyzing the global evolution of the outer electron belt during storms.

4. Jumping Particles

[32] To elucidate the impact of storm time magnetic field on the relativistic electron PSD we computed evolution of the third adiabatic invariant of one test particle from the dayside trapped population:

$$\Phi = \oint_{\Sigma} B_z dS = \oint_{\Sigma} \frac{B_0 R_E^3}{r^3} dS + \oint_{\Sigma} \Delta B_z dS \qquad (3)$$

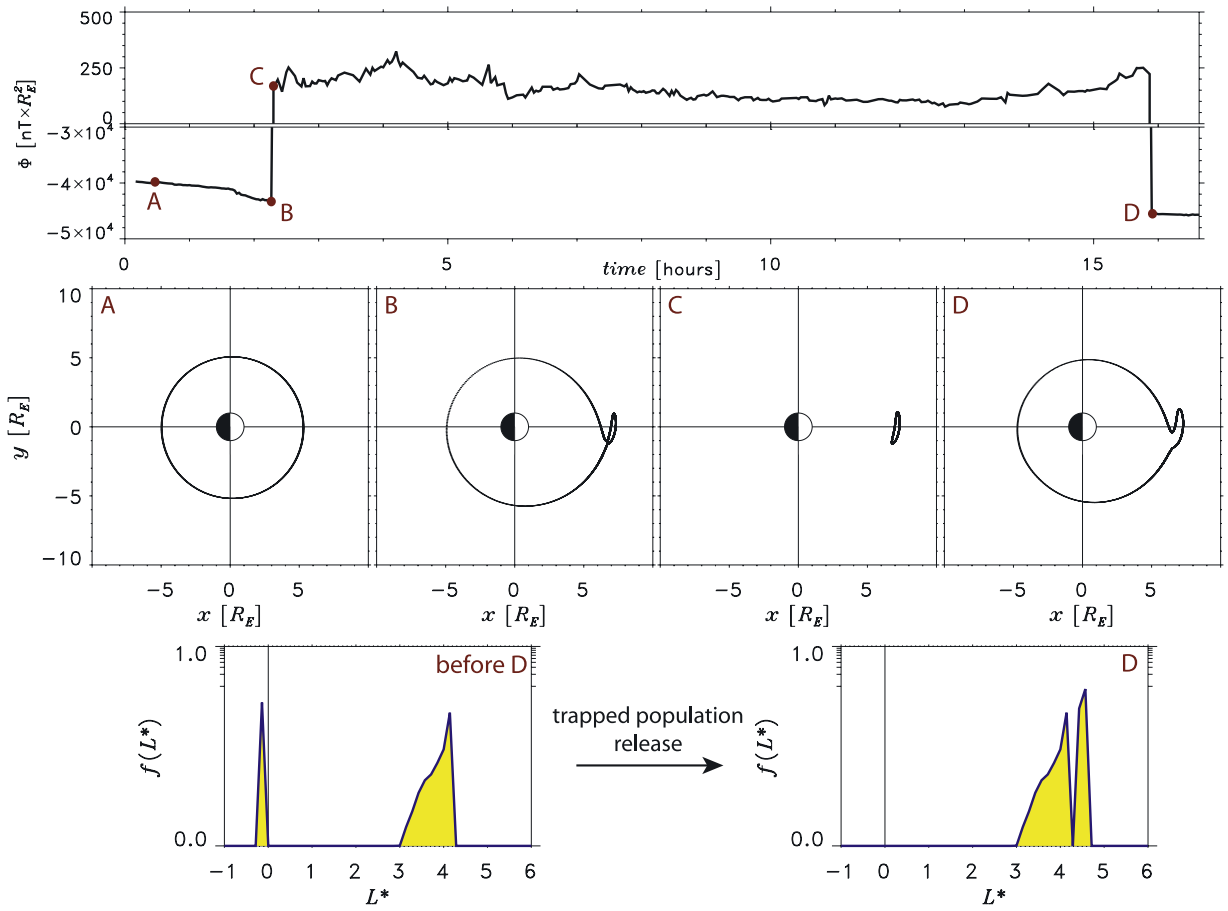

Figure 4. Jumping particles. (top) Time series of the third adiabatic invariant of one electron from the dayside trapped population. (middle) Electron orbit (a) before the storm onset, (b) prior to the trapping, (c) after the trapping, (d) after reinjection into the belt. (bottom) Radial profile of electron phase space density $f(L^*)$ before and after the release of the trapped population.

where Σ is the interior of electron's orbit, ΔB_z is the correction to the dipole term due to storm time current systems (output of the TS05). The results are summarized in Figure 4. The central panel of the figure shows electron drift trajectories in static magnetic magnetic field configurations calculated before the storm onset (A), prior to electron trapping (B), immediately after the trapping (C), and after electron release from the trap (D). The time series of the Φ is shown in the top panel of Figure 4. The invariant actually changes throughout the simulated period, varying in response to changes in the magnetic field. The most dramatic shifts of the invariant are associated with electron trapping and release. When first trapped, the electron is transferred from orbit (B) closed around the Earth to orbit (C) embedded in the dayside island. After the transition the dipole term on the right-hand side of equation (3), which was previously singular ($\mathbf{r} = 0 \in \Sigma_B$), becomes regular. As a result, total value of the invariant jumps discontinuously to a positive value. Conversely, when the electron is transferred back to a closed drift orbit (D) the dipole term becomes singular again and the invariant discontinuously acquires a negative value. Clearly, Φ is not an invariant of the motion under these conditions.

[33] The bottom panel of Figure 4 shows the radial profile of electron PSD calculated as a function of $L^* = -2\pi B_0 R_E^2/\Phi$ before and after the release of the dayside trapped population. The peak at negative L^* in the left plot is due to the trapped population. If represented as function of $\mathcal{L}$, which is not reflective of the third invariant during disturbed conditions, the same peak appears at $\mathcal{L} \simeq 7$ (see Figure 2 interval 5). As soon as particles are re-injected into the belt, the peak jumps to positive $L^* \simeq 4.5$ (see the right plot). Peak maximum of $\sim$0.1 corresponds to the prestorm PSD value at $L^* \simeq \mathcal{L} \simeq 6.0$ (see Figure 2), while at $L^* = 4.5$ the prestorm PSD has a negligent value of $<10^{-4}$. Thus electron reinjection led to a factor of 10^3 localized increase in electron PSD as compared to its prestorm values.

[34] It is generally believed that the shape of L^*-profile of electron PSD can be used to differentiate among acceleration mechanisms operating in the electron belt [e.g., *Green and Kivelson*, 2004]. Thus a localized peak in PSD at $L^* = 4-5$ is usually considered as an unambiguous indication of a local acceleration process, namely electron energization due to violation of the first adiabatic invariant μ via resonant wave-particle interaction [e.g., *Summers et al.*, 1998]. However, in our test-particle simulation we used the guiding center approximation in which $J = 0$ and $\mu = const$. Thus our results prove that localized peaks in PSD do not necessarily imply local electron acceleration and can be caused by large variations in the magnetic field. The storm

time distortion of the magnetic field that produces nonadiabatic drift orbit dynamics and nondiffusive transport appears to be a general feature of the storm time inner magnetosphere, so the appearance of peaks in PSD radial profiles should also be in general independent of the action of acceleration processes. It may therefore be necessary to critically examine whether the observed local radial PSD peaks are as unambiguous markers of local acceleration as has been thought.

5. Conclusion

[35] A test-particle simulation in the guiding center approximation was used in the analysis of transport and loss of relativistic electrons in the outer belt during the 7 September 2002 geomagnetic storm. The results show that the evolution of the magnetic field is one of the principal factors governing the global behavior of the storm time electron belt.

[36] By far the most prevalent effect is the prompt loss of the outer belt due to nonadiabatic transport to the magnetopause. Electron losses during storm main phase are associated with the Earthward expansion of the open-closed drift path boundary. Rapid enhancement of the partial ring current produces a large diamagnetic effect; the magnetic field intensity drops down to $\gtrsim 0$ nT in an extended region of the nightside magnetosphere. As a result electrons previously drifting around the Earth are transferred onto trajectories intersecting the magnetopause and are lost. In about 2.5 hours after the storm onset most of electrons from $L > 5$ were permanently lost from the belt.

[37] This result suggests that the outer belt for this storm did not undergo adiabatic expansion and recovery conventionally associated with the D_{st} effect. Rather, for this storm at least and most likely generally, the prestorm outer belt is lost and the poststorm outer belt electrons are a distinct population. Whether the outer belt fluxes are higher or lower following the storm therefore depends on the source intensity and inward transport and energization mechanisms so that one would not expect any consistent relationship between prestorm and poststorm flux levels.

[38] The solar wind time series exhibit variations in ULF frequency range which induce substantial electric fields over extended regions of the inner magnetosphere. While such global electric fields can be an important driver of electron motion at quiet geomagnetic conditions [*Ukhorskiy et al.*, 2006], the associated radial transport has characteristic timescales of $\gtrsim 10$ hours and therefore can be neglected at storm main phase as compared with rapid magnetopause losses.

[39] In addition to opening a large fraction of the outer belt electron drift paths, the distortion of the magnetic field due to the partial ring current also leads to topological transitions in the magnetic drift paths of relativistic particles. In the case of the 7 September 2002 storm this resulted in formation of an electron trap in the dayside magnetosphere. The trap was stable and held electrons for more than 11 hours of the storm. It collapsed due to the partial recovery of the ring current. Electrons were released back into the belt where they resumed their drift motion around the Earth.

[40] At trapping and release the third adiabatic invariant of electrons exhibits rapid jumps and changes sign. Thus before the release electron PSD had a radial profile monotonically increasing with L^* for all $L^* > 0$. After the release, however, the PSD profile showed a narrow peak around $L^* \simeq 4.5$. The result has two important implications. First, it shows that formation of localized structures in the L^*-profile of electron PSD does not necessarily require violation of either the first or the second adiabatic invariants. Second, the knowledge of the L^*-profile of electron PSD at a given moment of time is not sufficient to differentiate among global and local acceleration mechanisms. Proper analysis of acceleration/loss mechanisms at a given stage of a geomagnetic storm requires the knowledge of the history of PSD evolution from the storm onset.

[41] While it is clear that the inner magnetospheric magnetic field exhibits a dominant control on storm time evolution of the outer radiation belt, several important issues have to be addressed in future studies. In our analysis the consideration was restricted only to $\mu = const$ particles. However, during highly disturbed conditions, the distribution of magnetic field intensity exhibits large gradients which can violate the first adiabatic invariant of relativistic electrons. While most of test particles (>90%) conserved the first invariant throughout the storm, it is important to determine whether the particles that broke the invariant and therefore were removed from the simulation can produce any noticeable effects of the electron PSD.

[42] In the TS05 model the magnetopause location is calculated from the *Shue et al.* [1998] empirical model. Being an azimuthally symmetrical elliptical surface with location defined by a statistical fit to magnetopause crossings at similar solar wind conditions, the model magnetopause does not describe dynamical features such as magnetopause erosion, effects of Kelvin-Helmholtz instability, local time asymmetries and may not be accurate during extreme events. Thus it has to be analyzed at what extent the uncertainties in magnetopause location effect storm time magnetopause loss of radiation belt electrons described in the paper. The reported electron loss has also to be validated with data. Validation requires mapping of electron fluxes observed at various spacecraft to equatorial plane. Since electron motion is sensitive to the details of storm time magnetic field and its time variations, it is essential to use an accurate model of storm time magnetic field for the mapping procedure.

[43] It is also important to extend the simulation domain to $J \neq 0$ values. Complex distribution of storm time magnetic field can result in electron trapping off the equator which can increase the amount of electron flux reinjected into the belt at storm recovery phase.

[44] Finally, the influence of the dynamic magnetic field structure on repopulation of the outer belt needs to be considered to determine whether the nonadiabatic, nondiffusive processes identified here play a role in reformation of the outer belt.

[45] **Acknowledgments.** The research is supported by NSF grant ATM-0540121 and NASA grant NAG5-12722.

[46] Amitava Bhattacharjee thanks Reiner Friedel and another reviewer for their assistance in evaluating this paper.

References

Brautigam, D. H., and J. M. Albert (2000), Radial diffusion analysis of outer radiation belt electrons during the October 9, 1990, magnetic storm, *J. Geophys. Res.*, *105*, 291.

Chirikov, B. V. (1987), *Particle Dynamics in Magnetic Traps*, *Rev. of Plasma Phys.*, vol. 13, p. 1, Consult. Bur., New York.

Dessler, A. J., and R. Karplus (1960), Some properties of the Van Allen Radiation, *Phys. Rev. Lett.*, *4*, 271.

Dessler, A. J., and R. Karplus (1961), Some effects of diamagnetic ring currents on Van Allen Radiation, *J. Geophys. Res.*, *66*, 2289.

Elkington, S. R., M. K. Hudson, and A. A. Chan (2003), Resonant acceleration and diffusion of outer zone electrons in an asummetric geomagnetic field, *J. Geophys. Res.*, *108*(A3), 1116, doi:10.1029/2001JA009202.

Elkington, S. R., M. Wiltberger, A. A. Chan, and D. N. Baker (2004), Physical models of the geospace radiation enviroment, *J. Atmos. Sol. Terr. Phys.*, *66*, 1371.

Fok, M. C., T. E. Moore, and W. N. Spjeldvik (2001), Rapid enhancement of radiation belt electron fluxes due to substorm dipolarization of the geomagnetic field, *J. Geophys. Res.*, *106*, 3873.

Green, J. C., and M. G. Kivelson (2004), Relativistic electrons in the outer radiation belt: Differentiating between acceleration mechanisms, *J. Geophys. Res.*, *109*, A03213, doi:10.1029/2003JA010153.

Jordanova, V. K., and Y. Miyoshi (2005), Relativistic model of ring current and radiation belt ions and electrons: Initial results, *Geophys. Res. Lett.*, *32*, L14104, doi:10.1029/2005GL023020.

Li, X., et al. (1997), Multisatellite observations of the outer zone electron variation during the November 34, 1993, magnetic storm, *J. Geophys. Res.*, *102*, 14,123.

McIlwain, C. E. (1966), Ring current effects on trapped particles, *J. Geophys. Res.*, *71*, 3623.

Northrop, T. G. (1963), *The Adiabatic Motion of Charged Particles*, Wiley-Interscience, New York.

Nunn, D. (1993), A novel technique for ne numerical simulation of hot collision-free plasma; Vlasov Hybrid Simulation, *J. Comput. Ppys.*, *108*, 180.

Press, W. H., S. A. Teukolsky, W. T. Vetterling, and B. P. Flannery (1992), *Numerical Recipes in Fortran 77: The Art of Scientific Computing*, 2nd ed., Cambridge Univ. Press, New York.

Reeves, G. D., K. L. McAdams, R. H. W. Friedel, and T. P. O'Brien (2003), Acceleration and loss of relativistic electrons during geomagnetic storms, *Geophys. Res. Lett.*, *30*(10), 1529, doi:10.1029/2002GL016513.

Roederer, J. G. (1970), Dynamics of geomagnetically trapped radiation, in *Physics and Chamestry in Space*, edited by J. G. Roederer and J. Zahringer, vol. 2, Springer, New York.

Schultz, M., and L. J. Lanzerotti (1974), *Particle Diffusion in the Radiation Belts*, *Phys. and Chem. in Space*, vol. 7, Springer, New York.

Shprits, Y. Y., and R. M. Thorn (2004), Time dependent radial diffusion modeling of relativistic electrons with realistic loss rates, *Geophys. Res. Lett.*, *31*, L08805, doi:10.1029/2004GL019591.

Shue, J. H., et al. (1998), Magnetopause location under extreme solar wind conditions, *J. Geophys. Res.*, *103*, 17,691.

Summers, D., R. M. Thorne, and F. Xiao (1998), Relativistic theory of wave particle resonant diffusion with application to electron acceleration in the magnetosphere, *J. Geophys. Res.*, *103*, 20,487.

Tsyganenko, N. A., and M. I. Sitnov (2005), Modeling the dynamics of the inner magnetosphere during strong geomagnetic storms, *J. Geophys. Res.*, *110*, A03208, doi:10.1029/2004JA010798.

Ukhorskiy, A. Y., K. Takahashi, B. J. Anderson, and N. A. Tsyganenko (2006), The impact of ULF oscillations in solar wind dynamic pressure on the outer radiation belt electrons, *Geophys. Res. Lett.*, *33*, L06111, doi:10.1029/2005GL024380.

Volland, H. (1973), A semiempirical model of large-scale magnetospheric convection, *J. Geophys. Res.*, *78*, 171.

B. J. Anderson, P. C. Brandt, and A. Y. Ukhorskiy, Johns Hopkins University Applied Physics Laboratory, Johns Hopkins Road, Laurel, MD 20723-6099, USA. (aleksandr.ukhorskiy@jhuapl.edu)

N. A. Tsyganenko, Universities Space Research Association, NASA Goddard Space Flight Center, Code 612.3, Greenbelt, MD 20771-7925, USA. (nikolai.tsyganenko@gsfc.nasa.gov)